

Revisiting temperature sensitivity: How does Antarctic precipitation change with temperature?

Lena Nicola^{1,2,3}, Dirk Notz¹, and Ricarda Winkelmann^{2,3}

¹ Center for Earth System Research and Sustainability (CEN), Institute of Oceanography, Universität Hamburg, Germany

² Potsdam Institute for Climate Impact Research (PIK), Member of the Leibniz Association, P.O. Box 60 12 03, D-14412 Potsdam, Germany

³ University of Potsdam, Institute of Physics and Astronomy, Karl-Liebknecht-Str. 24-25, 14476 Potsdam, Germany

Correspondence: Lena Nicola (lena.nicola@pik-potsdam.de), Ricarda Winkelmann (ricarda.winkelmann@pik-potsdam.de)

Abstract. With progressing global warming, snowfall in Antarctica is expected to increase, which could counteract or even temporarily overcompensate increased ice-sheet mass losses caused by increased ice discharge, calving and melting. For sea-level projections it is therefore vital to understand the processes determining snowfall changes in Antarctica. Here we revisit the relationship between Antarctic temperature changes and precipitation changes, identifying and explaining regional differences and deviations from the theoretical approach based on the Clausius-Clapeyron relationship. Analysing the latest estimates from global (CMIP6) and regional (RACMO2.3) model projections, we find an average increase of 5.5 % in annual precipitation over Antarctica per degree of warming, with a minimum sensitivity of 2 % K⁻¹ near Siple Coast, and a maximum sensitivity > 10 % K⁻¹ at the East Antarctic Plateau region. This large range can be explained by the prevailing climatic conditions, with local temperatures determining the Clausius-Clapeyron sensitivity that is counteracted in some regions by the prevalence of the coastal wind regime. We compare different approaches of deriving the sensitivity factor, which in some cases can lead to sensitivity changes of up to 7 percentage points for the same model. Importantly, local sensitivity-factors are found to be strongly dependent on the warming level, suggesting that some ice-sheet models which base their precipitation estimates on parameterizations derived from these sensitivity factors might overestimate warming-induced snowfall changes, particularly in high-emission scenarios. This would have consequences for Antarctic sea-level projections for this century and beyond.

1 Introduction

Over the past decades, the Antarctic Ice Sheet has been losing mass at an accelerating pace (IMBIE Team, 2018; Rignot et al., 2019) and is increasingly contributing to sea-level rise (Fox-Kemper et al., 2021). Melting ice from the Antarctic Ice Sheet has risen global sea levels by 7.4 ± 1.5 mm between 1992 and 2020, caused by the total ice loss of 2671 ± 530 Gt over that period (Otosaka et al., 2022). Due to on-going melt, global sea levels are committed to rise for centuries to come (Levermann et al., 2013; Golledge et al., 2015).

The Antarctic Ice Sheet could however not only be a contributor to sea-level rise but may even slow down the rise in sea level by storing additional mass through increased snowfall (Seroussi et al., 2020). Antarctic precipitation is by far the most important positive contributor to the overall mass balance of the Antarctic Ice Sheet. The balance between snow accumulation

in the interior minus the surface ablation (wind transport, sublimation, very low surface melt) and the ice loss through calving
25 and sub-shelf melting determines the magnitude and pace of the Antarctic contribution to past and future global sea-level rise.

The uncertainty of the future Antarctic sea-level contribution in modelling studies generally arises both from the uncertainty
in the external (climate) forcing as well as from uncertainties in representing the governing processes and their relevant param-
eters in models (e.g., Rodehacke et al., 2020; Seroussi et al., 2020). Parts of this uncertainty arise from our limited understanding
how Antarctic precipitation is changing with warming and how the change in snowfall rates can be incorporated into ice-sheet
30 models. Addressing this uncertainty is the focus of this contribution.

Present-day observations of Antarctic precipitation are sparse and regional climate models disagree strongly in their es-
timates of annual surface mass balance (Mottram et al., 2021). For what is known, Antarctica is as dry as desert climates
(annual precipitation < 250 mm, Sikka, 1997) and is therefore often referred to as a *Polar desert*. Palerme et al. (2014) obtained
continent-wide snowfall rates through satellite-based radar and estimated a mean annual snowfall of 171 mm w.e. yr⁻¹ from
35 August 2005 to April 2011. Roussel et al. (2020) state an annual snowfall of roughly 186 mm w.e. yr⁻¹.

Most of the ice mass lies in the interior, but precipitation in Antarctica is concentrated at the ice-sheet margins. Annual
precipitation is exceeding 1000 mm w.e. yr⁻¹ in coastal parts of West Antarctica, near Wilkes Land as well as at the Antarctic
Peninsula (see Panel (a), left, Fig.1). In the interior of the ice sheet, mean annual precipitation is below 50 mm w.e. yr⁻¹.

Despite the little annual snowfall, mass gains through snowfall have exceeded mass losses from the Antarctic Ice Sheet
40 between 2003-2008 (Zwally et al., 2015). Model simulations show that Antarctic snowfall may increase significantly in a
warming climate, and could thus partly buffer the warming-induced ice loss (Bracegirdle et al., 2008; Frieler et al., 2015;
Rodehacke et al., 2020). While insignificant changes of snowfall were reported from 1957 to 2006 (Monaghan et al., 2006),
Medley and Thomas (2019) find that snow accumulation has been increasing by 1.1 mm w.e. per decade between 1901 and
2000 and by 2.5 mm w.e. per decade after 1979, mitigating sea-level rise by about 10 mm since 1901.

It can be hypothesised that Antarctic snowfall increases with temperature according to the Clausius-Clapeyron relationship
45 (Clapeyron, 1834; Clausius, 1850), describing the saturation water vapour pressure, e_s , as a function of temperature, T . This
hypothesis is based on the assumption that Antarctic precipitation is solely driven by temperature and the associated availability
of moisture in the atmosphere. Under this assumption, Antarctic snowfall increases with the same sensitivity as the general
capacity of the air to hold moisture, which is given by the saturation water vapour pressure, e_s , beyond which water vapour con-
50 densates and can thus potentially precipitate as snow in Antarctica. Held and Soden (2006) introduce the Clausius-Clapeyron
relationship as

$$\frac{d \ln e_s}{dT} = \frac{L}{R_v T^2} \equiv \alpha(T) \quad (1)$$

with L being the latent heat of vaporization and R_v the specific gas constant for water vapour. $\alpha(T)$ in Equation (1) is the
sensitivity parameter, translating the change in temperature into a relative change in saturation water vapour pressure. With
55 $L = 2.5 \times 10^6 \text{ J kg}^{-1}$, $R_v = 461 \text{ J K}^{-1} \text{ kg}^{-1}$ and a mean temperature of the lower troposphere where the moisture resides of
about $T = 260 \text{ K}$ (e.g. Hartmann, 2016), the global scaling factor lies at around $8 \% \text{ K}^{-1}$. If we were to use the continent-wide
Antarctic mean annual surface air temperature of $T_g = -33.6 \text{ }^\circ\text{C}$ (239.6 K, 1981-2000 mean of ERA5-Land reanalysis data),

the sensitivity factor, $\alpha(T_g)$ would be calculated as $9.4 \% \text{ K}^{-1}$. However, such calculation using surface air temperatures is biased, because changes in the surface temperature T_g are larger than changes in the temperature of the moisture-holding free atmosphere above the prevailing surface inversion layer (Jouzel and Merlivat, 1984; Connolley, 1996). Fortuin and Oerlemans (1990) suggest that the temperature of the free atmosphere above the inversion in Antarctica, T_f , can be approximated from the surface temperature T_g (in Kelvin), as

$$T_f[K] = 0.67 \cdot T_g[K] + 88.9. \quad (2)$$

Using this approximation, the theoretically obtained sensitivity $\alpha(T)$ from Eq. 1 yields $8.7 \% \text{ K}^{-1}$, for a surface air temperature of $T_g = 239.6 \text{ K}$ (1981-2000 mean of ERA5-Land reanalysis data). We will use this bias-corrected value throughout this paper as an estimate of the continent-scale mean sensitivity for a change in today's surface temperature. For the model simulations, we will analyse the sensitivity directly relative to the modelled change in surface temperature, as this temperature is (a) more readily available from observations and the model simulations and (b) has been the standard measure also in previous studies. An additional correction for the temperature of the moisture holding layer of the atmosphere is not necessary in this case, as the models resolve the vertical temperature changes in their atmospheric thermodynamic schemes.

Projections of regional climate models show a wide range of snowfall changes in the coming decades depending on the model input (Kittel et al., 2021). Simulations of the regional model RACMO2.3, which is often used as input of numerical ice-sheet models (e.g. in Garbe et al., 2020; Seroussi et al., 2020), project that mean annual Antarctic precipitation will increase from approximately $189 \text{ mm w.e. yr}^{-1}$ in 1981-2000 to $289 \text{ mm w.e. yr}^{-1}$ at the end of the century for the SSP5-85 scenario. This corresponds to an increase by $+52.43\%$ for the simulated mean temperature increase of 6.7 K . In these simulations, precipitation increases most in coastal areas, but also rises in the interior (Fig. 1(a), right panel). We note that the temperature and the precipitation increase in RACMO2.3 can be considered as a very high estimate of the expected changes, because the climate model CESM2 that is used to provide lateral boundary conditions for RACMO2.3 has an unrealistically high climate sensitivity (Gettelman et al., 2019).

Global coupled climate models participating in the Coupled Model Intercomparison Project Phase 6 (CMIP6) show differently strong responses of Antarctic precipitation to temperature changes in the 21st-century, depending both on the underlying future climate scenario and the specific models. To examine the spread across different future climate scenarios, we analyse the expected changes for three shared-socioeconomic pathway (SSP) - scenarios for characterising future climatic conditions in Antarctica: SSP1-26 as a low emission, SSP2-45 as intermediate and SSP5-85 as a high emission scenario (Riahi et al., 2017). End-of-century (2081-2100) Antarctic surface-air temperatures are projected to change relative to present-day conditions (1981-2000) by $1.6 \pm 0.8 \text{ K}$, $2.7 \pm 0.9 \text{ K}$ and $4.7 \pm 1.4 \text{ K}$, for the low (SSP1-26), intermediate (SSP2-45) and high emission scenarios (SSP5-85). For these temperature changes, annual precipitation is projected to increase by $9.7 \pm 7.3 \%$, $15.8 \pm 8.1 \%$, and $28.8 \pm 12.6 \%$, respectively.

Because it is numerically expensive and technically challenging to couple global atmosphere-ocean general circulation models to an interactive ice sheet, standalone ice-sheet models are usually used that often employ a scaling approach to translate changes in air temperature to changes in Antarctic precipitation. In ice-sheet models, precipitation can be scaled with

temperature or temperature anomalies, using sensitivity factors ($\% K^{-1}$) given by the existing literature. This approach is often used in long-term projections, where regional climate model estimates are not available: Albrecht et al. (2020) for instance used different values for the sensitivity factor to perform glacial-cycle simulations and to test for parameter sensitivity. Quiquet et al. (2018) scale the surface mass balance with a sensitivity factor, assessing Antarctic Ice Sheet changes for the last 400 kyr. Huybrechts (2002) deduce the precipitation and basal melt rate from simple temperature relationships for performing glacial cycle simulations. Rodehacke et al. (2020) scale precipitation with temperatures, estimating Antarctica's sea-level contribution when using different precipitation parameterizations such as CMIP5 model output or constant scaling factors inside the ice-sheet model.

100 Generally, snowfall in Antarctica depends on a complex interplay of processes. Not only moisture availability and temperature play a crucial role, but also the local wind regime (Grazioli et al., 2017), the occurrence of atmospheric rivers, and large scale atmospheric variability (Nicolas et al., 2017; Wille et al., 2019; Eayrs et al., 2021; Maclennan et al., 2022). Also the detailed vertical temperature structure of the atmosphere, the density profile of the air and the resulting catabatic winds, the distance from the coast, the surface slope and the surface shape are of relevance (Fortuin and Oerlemans, 1990). In addition, 105 synoptic scale features, such as cyclones and fronts, generally influence coastal precipitation (Bromwich, 1988). The large-scale, integrated, long-term evolution of precipitation is, however, found to be generally dominated by thermodynamic changes (Uotila et al., 2007; Krinner et al., 2014; Grieger et al., 2016).

It is known that the Antarctic Ice Sheet may gain mass under warming due to increased snowfall. Such increase is expected to generally follow a given rise in temperature according to the Clausius-Clapeyron relationship. Already Robin (1977) has 110 proposed a linear relationship between water vapour pressure over ice and temperature, whilst concluding that this is "an empirical approximation to observations, rather than a natural law". Two of the earliest studies performing regression analyses with accumulation data were Muszynski and Birchfield (1985) and Fortuin and Oerlemans (1990), with the latter study analysing, among others, analytically how atmospheric stratification and the surface topography impact moisture availability and thus regional precipitation. Krinner et al. (2007), Bengtsson et al. (2011), Ligtenberg et al. (2013) or Agosta et al. (2013) 115 use changes in surface mass balance (SMB) to estimate sensitivity factors between precipitation and temperature, while Frieler et al. (2015), Fudge et al. (2016) and Medley and Thomas (2019) use changes in snow accumulation to derive relative changes in snowfall per degree of warming ($\% K^{-1}$). Other studies have determined a sensitivity of net precipitation to warming, meaning precipitation minus evaporation (commonly denoted P-E), to also account for an increase in evaporation rates (Uotila et al., 2007; Bracegirdle et al., 2008). Palerme et al. (2017) use changes in total precipitation (P) estimates, focusing on the increase 120 of snowfall (+ rain) with warming. Several more studies have analysed a potential connection of mass gains and atmospheric warming, see Fig. 1, but have not estimated a sensitivity factor in the form that is discussed here ($\% K^{-1}$). As data sources for estimating the sensitivity of precipitation, existing studies have incorporated ice core data (Petit et al., 1999; Van Ommen et al., 2004; Frieler et al., 2015; Fudge et al., 2016), ice core data combined with reanalysis (Medley and Thomas, 2019), AOGCM output partaking in early CMIP initiatives (Uotila et al., 2007; Bracegirdle et al., 2008), CMIP3 (Gregory and Huybrechts, 2006; Krinner et al., 2014) and CMIP5 (Frieler et al., 2015; Grieger et al., 2016; Palerme et al., 2017; Rodehacke et al., 2020), 125 or high-resolution, regional or paleoclimate model output (Krinner et al., 2007; Agosta et al., 2013; Ligtenberg et al., 2013;

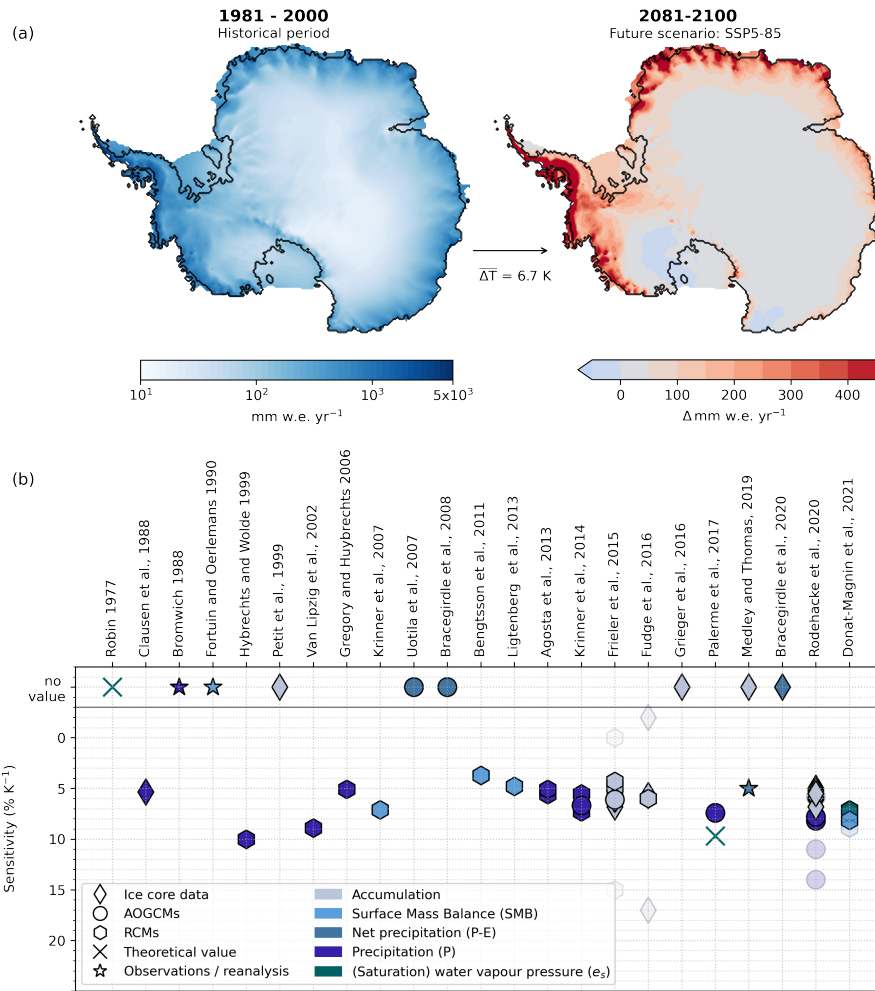


Figure 1. How is Antarctic precipitation changing with warming? (a): Change in mean annual precipitation as simulated with the regional climate model RACMO2.3 (left) for the historical period (1981-2000) and (right) projected for the end of this century (2081-2100) under a high-emission scenario (SSP5-85). On average, Antarctic-wide temperatures change by 6.7 K between the two time periods. (b): Literature values from ice-core data (diamonds), AOGCMs (circles), RCMs (hexagons) as well as observations/reanalysis (stars), for the sensitivity of precipitation, net precipitation, accumulation and surface mass balance (often linked to the sensitivity of saturation water vapour pressure) to warming (given in $\% K^{-1}$). Upper row shows studies assessing the relationship but without quantifying such sensitivity factor. Translucent markers indicate extreme values found for example within ice cores (Fudge et al., 2016) or in modelling results (Frieler et al., 2015; Rodehacke et al., 2020; Donat-Magnin et al., 2021).

Krinner et al., 2014; Frieler et al., 2015; Donat-Magnin et al., 2021). Overall, the sensitivity factors assessed from the literature vary roughly between 4 and 10 $\% K^{-1}$, see Fig. 1, with extreme values for the change in snow accumulation found in parts of ice cores (Fudge et al., 2016) and certain modelling studies (Frieler et al., 2015; Donat-Magnin et al., 2021).

130 In this paper, we update previous continent-wide estimates of the sensitivity factors of Antarctic precipitation to temperature based on the latest available model data and reconcile it with previous approaches (Section 3). We show how and explain why these sensitivity factors differ strongly across the ice sheet (Section 4). We conclude that the scaling approach often used in ice-sheet models should be revised, depending on the chosen application.

2 Methods

135 In our study we revisit the temperature-dependency of snowfall changes on the Antarctic Ice Sheet. We use a least-squares regression analysis to determine the sensitivity factor α that describes how Antarctic precipitation is changing with temperature. This approach follows the general definition of the Clausius-Clapeyron relationship (Eq. 1). Sensitivity factors have been commonly estimated using relative changes of precipitation or accumulation (changes in % compared to a reference period) and values of warming (ΔT , e.g. Frieler et al., 2015; Fudge et al., 2016; Palerme et al., 2017). For example, Frieler et al. (2015)
140 use changes in warming and relative changes in precipitation compared to 1850-1900. Krinner et al. (2007), Krinner et al. (2014) and Palerme et al. (2017) compare changes between two states, e.g. the end of the 20th-century versus the end of the 21st-century.

In our analysis, we follow the Clausius-Clapeyron theory (Eq. 1) more closely, applying the regression analysis to log-scaled mean annual precipitation and the annual temperature time series. This makes our approach independent of the chosen
145 reference period. Donat-Magnin et al. (2021) use a similar approach, but they do not account for the full length of the available timeseries. As discussed above, for the model simulations we analyse sensitivities only as a function of mean annual surface air temperatures, as the models implicitly resolve the impact of the vertically varying temperature profile in their calculation of precipitation.

We perform a sensitivity analysis in three ways:

- 150 1. Continent-wide temporal regression - We first average over available temperature and precipitation fields (weighted by surface area) across the entire Antarctic continent and then obtain a sensitivity value from the least-squares regression of the time series of continent-wide annual temperature and log-scaled precipitation. To compare our results to previous studies, we repeat a temporal regression using precipitation anomalies relative to a reference period (linear regression).
- 155 2. Grid-point temporal regression - We first perform the least-squares regression with the local time series of annual temperature and log-scaled precipitation for every grid point. In this regression the predictor arrays are the time series of temperature for each grid point respectively. This yields a spatial distribution of scaling factors. For comparing these estimates to the continent-wide temporal regression, these grid values are averaged over the ice sheet (area-weighted).
- 160 3. Spatial regression - For each time slice of the available data $(x,y,time)$, we perform a least-squares regression with the data points from the spatial distribution of temperature and log-scaled precipitation (x,y) . Here the predictor values are the 1440X1080 (lonxlat) grid points of temperature values for each time slice. The regression with the 1440x1080 grid points of precipitation then yields a new estimate of the sensitivity of how Antarctic precipitation follows local

temperatures across the ice sheet. For analysing the change in this sensitivity with temperature, we perform a temporal regression of the scaling factors with the mean annual temperature time series. This second step makes this approach distinct from the grid-point regression where only a temporal regression is performed.

165 Our analysis is based on different types of data to robustly delineate the sensitivity of Antarctic precipitation to temperature under present-day conditions, as well as their potential changes in the future.

While direct measurements are scarce and observational products such as the CloudSat data lack the needed resolution (Palerme et al., 2014), we use the ECMWF ERA5-Land reanalysis data (Muñoz Sabater, 2019) as a best estimate of present-day conditions in Antarctica. These reanalysis data provide spatially and temporally complete coverage of the historical and
170 present-day evolution of precipitation and temperature patterns for Antarctica. The ERA5-Land reanalysis is provided through the Copernicus Climate Change Service (C3S) at the ClimateData Store and is available at a resolution of $0.1^\circ \times 0.1^\circ$ on a lon-lat grid at hourly resolution. We here use monthly averaged variables.

In addition, we analyse CMIP6 model data which is available from Earth System Grid Federation (ESGF, for example at <https://esgf-data.dkrz.de>). We combine historical data that covers the period of 1850-2014 with projections for the years
175 2015 to 2100. A few models provide projections until the year 2300, including for the low-emission SSP1-26 scenario models CanESM5, IPSL-CM6A-LR, MRI-ESM2-0, and UKESM1-0-LL, and additionally for the high-emission SSP5-85 scenario models ACCESS-CM2 and MIROC-ES2L. We use the first available ensemble member of each CMIP6 model for analysis. The nominal resolution of the CMIP6 ensemble differs substantially and lies between 50 km (CNRM-CM6-1-HR and GFDL-CM4) and 500 km (CanESM5). If possible we use the native model mask (through variable *sftlf*) to extract data for the Antarctic
180 continent. For analysing the regional CMIP6 model mean of sensitivity factors, we regrid all models to a common 1440x1080 grid, following the highest resolution of the available models (GFDL CM4). We incorporate more than 30 different models for the analysis until 2100.

Adding to that, we use mean monthly values of near-surface temperature and precipitation data from the regional model RACMO2.3 for the years 1950 to the end of the 21st-century (van Meijgaard et al., 2008; Van Wessem et al., 2018). For the
185 future period 2015-2100, RACMO2.3 is here forced with CESM2 model output for the SSP5-85 scenario, which, as discussed above, might have given rise to too high estimates of future warming. The data is available at a 27 km resolution.

We analyse the full time series of yearly mean temperature and precipitation until the year 2100 (and in some cases until 2300). In order to obtain a 20th-century and a 21st-century reference period, we average values over the years 1981-2000 and 2081-2100, respectively. We use a twenty year average to reduce the impact of internal variability, following the approach in
190 the recent IPCC AR6 WG1 report (Masson-Delmotte et al., 2021). Mean values of both time windows will be used to assess sensitivity factors as in Palerme et al. (2017).

3 Continent-wide scaling factors from regional and global climate model data

Analysing Antarctic temperature and precipitation from all available CMIP6 models over the time period 1850-2100, we find a sensitivity of Antarctic precipitation to temperature of approx. $\alpha = 5.5\% \text{ K}^{-1}$, which is independent of the chosen

195 climate-change scenario and close to previous estimates. The statistical means across all individual CMIP6 sensitivities from the continent-wide temporal regression are $5.5 \pm 1.2 \% K^{-1}$, $5.5 \pm 1.1 \% K^{-1}$ and $5.5 \pm 0.9 \% K^{-1}$ using the historical period and the three SSP-scenarios respectively (SSP1-26, SSP2-45, SSP5-85). Using the inter-model mean of Antarctic precipitation and temperature results in slightly higher values of $\alpha = 6.2 \% K^{-1}$, $5.9 \% K^{-1}$ and $5.7 \% K^{-1}$, see Fig. 2. RACMO2.3 data give a sensitivity factor of $\alpha = 6.4 \% K^{-1}$ using the SSP5-85 scenario with the available historical period from 1950
200 to 2100. $6.4 \% K^{-1}$ lies close to the upper end of the inter-model spread of the CMIP6 ensemble for the SSP5-85 scenario ($5.5 \pm 0.9 \% K^{-1}$) and the deviation could thus generally be explained by differing model climate sensitivities.

The R^2 -values of the performed temporal regressions with the CMIP6 model data are generally highest for the SPP5-85 scenario with R^2 up to 0.94 for models CESM2-WACCM, CNRM-CM6-1-HR and CanESM5, see Fig. 2 for details. These high values of R^2 in the high emission scenario arise probably from the high signal to noise ratio that is obtained through the
205 high warming rates in SSP5-85. Note that at the time of our analyses not all CMIP6 models provided all future scenarios. All model-specific scaling factors are summarised in Table A1 in the Appendix. For the RACMO2.3 data we obtain a R^2 value of 0.92.

Our sensitivity factor of approx. $5.5 \% K^{-1}$ as the average across CMIP6 models is slightly lower than the CMIP5 estimate of $6.1 \% K^{-1}$ derived in Frieler et al. (2015). This can in parts result from differences in the CMIP6 versus the CMIP5 ensemble
210 (Zelinka et al., 2020; Payne et al., 2021). Moreover, as described above we are using a log-based approach here rather than relative anomalies which also leads to slightly different estimates. Using the same approach as in Frieler et al. (2015) (i.e., anomalies wrt. 1890–1980), we obtain a mean sensitivity of $5.9 \pm 1.3 \% K^{-1}$. Individual model results from this analysis are shown in Appendix Fig. A2. Quantifying the changes between the two reference periods, i.e., the end of the 20th vs. the end of the 21st-century, results in a higher sensitivity of $7.3 \% K^{-1}$, see Fig. A3, which is close to the CMIP5 estimate in Palerme
215 et al. (2017). This shows that the calculated sensitivity depends on the chosen analysis method.

For the extended CMIP6 projections until 2300, we use the model output by ACCESS-CM2, CanESM5, IPSL-CM6A-LR, MIROC-ES2L, MRI-ESM2-0 and UKESM1-0-LL. For these models we find sensitivities between 4.1 and $6.5 \% K^{-1}$ dependent on the model and the chosen scenario, see Fig. 3. We find that the old approach of estimating sensitivity factors from changes relative to a reference period shows a stronger bias for the SSP5-85 scenario, compare Appendix Fig. A2.
220 The sensitivity factors for e.g. the CanESM5 model results in $13.3 \% K^{-1}$ for a linear temporal regression compared to $6.3 \% K^{-1}$ in our logarithmic approach. The difference is due to the nature of the regression itself. With a simple linear regression using anomalies, we approximate the exponential function with percentage changes, which only holds for very small changes in the predictor variable, here increments of warming (ΔT). If the chosen model shows strong warming, hence large ΔT , the regression becomes inaccurate. Using output from climate models that show strong warming rates, i.e. that have a high
225 equilibrium climate sensitivity, such as CanESM5 (Meehl et al., 2020), the relative anomaly approach thus significantly alters the results from the multi-model analysis. Our logarithmic approach on the other hand incorporates the exponential function directly in the regression analysis; this avoids a potential bias towards the models with higher climate sensitivity (sometimes referred to as the "hot model problem", see e.g. Hausfather et al. (2022)).

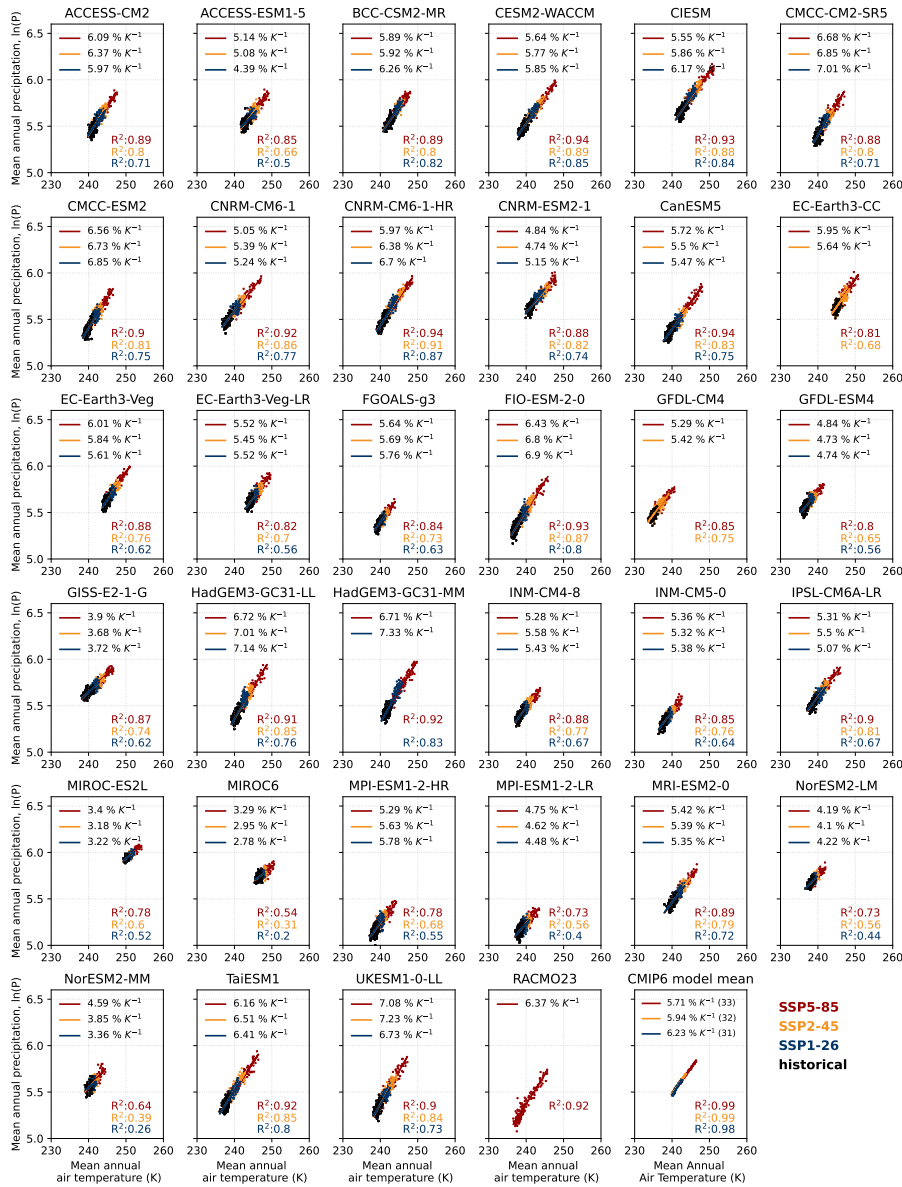


Figure 2. Update on continent-wide scaling factors based on CMIP6 and RACMO2.3 21st-century projections. Sensitivity factors are estimated over the period 1850-2100 for the CMIP6 ensemble by combining the historical period with three available shared-socioeconomic pathway scenarios (SSP1-26, SSP2-45 and SSP5-85), and over the period 1950-2100 for RACMO2.3. For the CMIP6 model mean, the numbers in brackets refer to the number of models incorporated into the analysis.

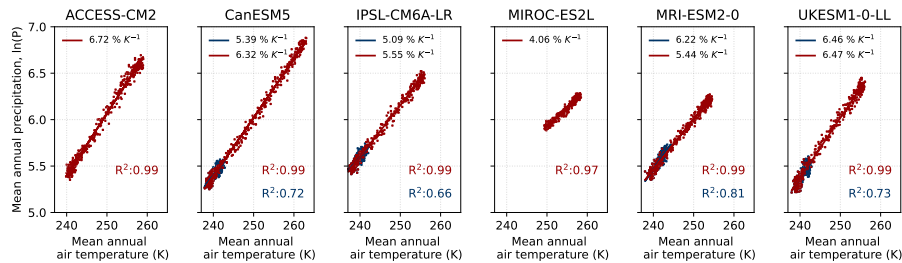


Figure 3. Continent-wide scaling factors for CMIP6 models simulating Antarctic climate change until 2300. Red colors refer to shared-socioeconomic pathway SSP5-85, blue colors refer to shared-socioeconomic pathway SSP1-26.

4 Regional sensitivity factors differ across the ice sheet

230 Performing the grid-point temporal regression of available CMIP6 model data shows that, across the ice sheet, sensitivity factors in certain regions are substantially different from the continental scaling factor of approximately $5.5 \% \text{ K}^{-1}$ obtained in the previous section, see Fig. 4. This largely confirms findings by Rodehacke et al. (2020), showing that regional sensitivities can differ substantially from the continent-wide scaling also in CMIP5. Note that we here use the time period of 1950-2100 to compare the spatial sensitivities with the results from RACMO2.3 (which are available for the same time period). Using the

235 period from 1850 to 2100 only causes very minor differences in our results.

The spatial sensitivities obtained from the multi-model mean of the regridded temperature and precipitation fields show similar patterns across the different SSP-scenarios: In the Ross ice-shelf region there are very low sensitivity factors while in the interior, factors go up to more than $10 \% \text{ K}^{-1}$. Sensitivity factors are on average around 2% higher in East Antarctica than in West Antarctica (here given roughly by the $40^\circ \text{ W} / 320^\circ \text{ E}$ and $180^\circ \text{ W} / \text{E}$ longitudes as lateral boundaries). We here

240 acknowledge more sophisticated ice dynamical definitions i.e. that are derived from ice divides of individual ice drainage basins (Rignot et al., 2011; Zwally et al., 2012). For the three chosen SSP-scenarios, the mean area-weighted factors are 7.7, 7.4, and $7.2 \% \text{ K}^{-1}$ for East Antarctica and 5.7, 5.4 and $5.3 \% \text{ K}^{-1}$ for the West Antarctic Ice Sheet, respectively. The mean R^2 -values for the EAIS are higher than for the WAIS ($R^2 = 0.79, 0.86, 0.94$ vs. $R^2 = 0.64, 0.72, 0.85$ for the respective future scenarios, compare Appendix Fig. A4). The difference between the two ice sheets could result from the low sensitivity factors found

245 near Siple Coast, where the temporal regression performs very poorly and skews the mean for the WAIS to lower values. This could be for instance due to a prominent area of converging katabatic winds (Parish and Bromwich, 2007), that could diminish precipitation at the coast (Grazioli et al., 2017), or generally hints at the large imprint of dynamic atmospheric systems in the area.

Comparing sensitivity factors across the ice sheet with the respective present-day temperatures (see Fig. A1 in the Ap-

250 pendix), allows us to explain much of the spatial patterns: Higher sensitivity factors are generally found in regions with lower temperatures. This is consistent with the theory, as the Clausius-Clapeyron relationship in Eq. (1) gives higher values of α for colder temperatures. Local temperatures especially in East Antarctica can reach well below the mean annual air temperature of

239.6 K / -33.6 °C (1980-2000 mean from ERA5-Land reanalysis). This temperature results in a theoretical sensitivity factor of 8.7 % K⁻¹ when correcting for the slower warming of the atmosphere compared to the surface (see above). This estimate is
255 consistent with the sensitivity factors we find in the cold Antarctic interior, see Fig. 4. In general, the relationship between local temperatures and sensitivity factors is most pronounced on the East Antarctic plateau where the influence of coastal winds is considered to be less significant (Bromwich, 1988). The effect of a more continental climate is supported by ice core studies from Law and Taylor Dome in East Antarctica: Van Ommen et al. (2004) show that during the LGM, the local climate was closer to present-day central Antarctica as glacial accumulation rates were more closely tied to saturation vapour pressure than
260 in the Holocene.

While the overall spatial pattern is robust for the different climate change scenarios, the sensitivity factors are generally lower for the high-emission SSP5-85 scenario, and higher for the low-emission SSP1-26 scenario. This tendency can be seen in the local factors across the ice sheet, with the difference between scenarios being particularly pronounced in East Antarctica. The tendency of lower sensitivity factors for higher emissions is even more apparent when averaging over the scaling factors
265 for each scenario (see Panel (c) in Fig. 4): we find a mean area-weighted scaling factor of 7.2, 6.9 and 6.7 % K⁻¹ for SSP1-26, SSP2-45 and SSP5-85 scenario, respectively. This is consistent with the RACMO2.3 mean scaling factor of 7.5 % K⁻¹ for the SSP5-85 scenario.

This mean of the spatially resolved sensitivity factors of the CMIP6 model data is thus higher than the continent-wide estimate of 5.5 % K⁻¹, which was independent of the chosen warming scenario. (Note the difference between the mean of
270 the grid-point scaling factors and the continent-wide scaling factor, see methods section). This difference in sensitivity factors is due to the non-linearity (logarithmic relationship). Local differences are diminished when generating the continent-wide temperature and annual precipitation time series. For the RACMO2.3 model we find small regions of high sensitivity factors in parts of Dronning Maud Land and around the Filchner-Ronne Ice Shelf that are not visible in the CMIP6 model results, see Fig. 4. We believe this is due to local dynamic effects which are incorporated in the regional climate models and are not resolved in
275 the CMIP6 models. This is consistent with regional studies, finding scaling factors of 7.4 to 8.9 % K⁻¹ for the Amundsen Sea region (Donat-Magnin et al., 2021).

We find an even stronger difference between a 'cold' and a 'warm' future scenario when examining the local sensitivity factors from those models that simulate Antarctic precipitation and temperature until 2300 (see Fig. 5). The results of the low-
(SSP1-26) and high emission scenario (SSP5-85) show a strong difference in temperature sensitivities across the ice sheet. For
280 the SSP1-26 scenario, the area-weighted mean scaling factors across the ice sheet are > 8 % K⁻¹. For the warmer SSP5-85 scenario, we find much lower sensitivities. The differences in the area-weighted mean scaling factors between the two scenarios lie between 0.9 % K⁻¹ for CanESM5 and 2.9 % K⁻¹ for the MRI-ESM2-0 model. Here the CanESM5 model shows local warming of > 30 K by 2300 compared to present day, which leads to a strong reduction in sensitivity as expected from the definition of α .

285 Our results highlight that when simulating changes in Antarctic mass balance in the future, we need to consider these local sensitivities of precipitation change to warming. Using spatially resolved scaling factors that depict the local conditions could improve projections of the Antarctic sea-level contribution.

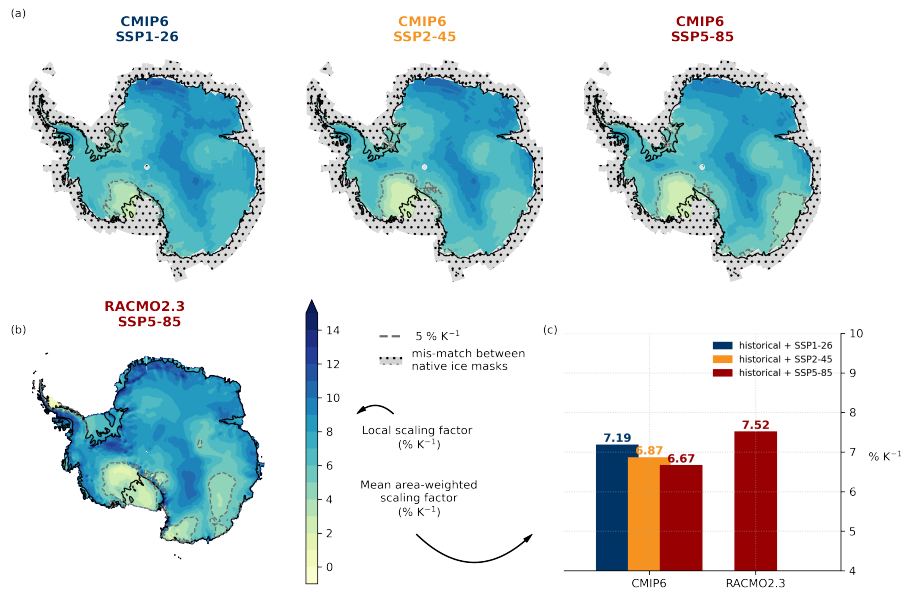


Figure 4. Sensitivity factors across the ice sheet derived from 21st century projections. (a) Spatially-resolved sensitivities for the CMIP6 model mean for each SSP scenario. The point-wise temporal regression is based on the period 1950 to 2100 by combining the historical period with the SSP1-26, SSP2-45 and SSP5-85 future scenarios, respectively. (b) Spatially-resolved sensitivities for RACMO2.3 model data, which was forced by CESM2 with SSP5-85 forcing (1950-2100). Dashed lines in maps indicate the $5\% \text{ K}^{-1}$ contour line, which refers to a commonly used sensitivity factor in ice-sheet modelling, such as in Garbe et al. (2020). Hatched regions shows a mis-match between native ice masks of the CMIP6 ensemble which is excluded from the analysis. (c) Comparison of area-weighted mean sensitivities, averaged over the same area of interpolated CMIP6 and RACMO2.3 data.

As we find that local sensitivity-factors depend on the warming level, ice-sheet models which base their precipitation projections on parameterizations derived from these sensitivity factors might overestimate warming-induced snowfall changes, particularly in high-emission scenarios.

5 Discussion and conclusion

The Clausius-Clapeyron equation suggests a clear relationship between changes in temperature and in the moisture-holding capacity of the air, which can potentially be translated into a relationship between changes in temperature and precipitation. Our study amends the existing literature by analysing the regional and continent-wide scaling factors obtained from the latest available model data from regional model RACMO2.3 and the CMIP6 model ensemble.

Overall, we find that the suite of formerly applied methods to establish the sensitivity of potential precipitation changes in Antarctic for a given amount of warming yield different results. Especially when analysing high-end scenarios with strong changes in annual air temperatures, multi-model mean values can be skewed if the sensitivity factors are calculated through

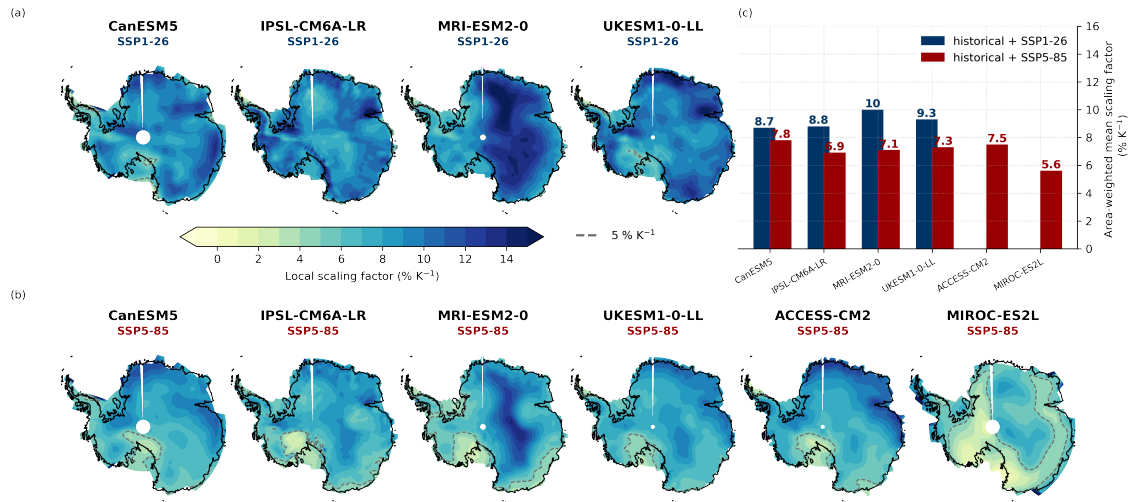


Figure 5. Sensitivity factors across the ice sheet derived from projections until 2300. Results are given for individual CMIP6 models that were run until the year 2300 for (a) SSP1-26, and (b) SSP5-85. Dashed lines in maps indicate the 5 % K⁻¹ contour line, which refers to a commonly used sensitivity factor in ice-sheet modelling, such as in Garbe et al. (2020). (c) Comparison of area-weighted mean sensitivities.

relative changes to a fixed reference period. When using a logarithmic approach for the temporal regression analysis, we generally obtain more robust results, because the Clausius-Clapeyron relationship is logarithmic by nature.

Across all considered SSP scenarios for the period 1850-2100, local scaling factors obtained through grid-point wise temporal regression can exceed 10 % K⁻¹, while continent-wide scaling factors from annual mean temperatures and precipitation only yield approximately 5.5 % K⁻¹ for all scenarios. This value lies substantially below the theoretical value of 8.7 % K⁻¹ for the 20th century reference period (see above). This discrepancy highlights the necessity to use spatially resolved sensitivity factors when scaling local precipitation patterns into the future.

Moreover, Van Ommen et al. (2004) and Fudge et al. (2016) find a temporally varying relationship between temperature and accumulation rate in ice core data. Assuming one constant scaling factor may hence not capture an evolving scaling relationship through space and time.

While the change in precipitation in the interior of the Antarctic continent follows the theory quite closely, the scaling factors near the coast can be substantially lower. This can be explained by the presence of a pronounced coastal wind regime that substantially affects local precipitation (Grazioli et al., 2017; Lemonnier et al., 2019). This gets evident when performing a *spatial* regression with present-day temperature and precipitation fields. When analysing to which degree the regional temperature distribution can explain the regional distribution of precipitation rates across the ice sheet, we find that the temperature pattern in Antarctica can explain roughly 83 % of the annual precipitation when assuming a direct relationship between the temperature and precipitation fields. This estimate is similar to the value of 72 % explained variance calculated by Fortuin and Oerlemans (1990) for the interior of the ice sheet. Similarly to their study, we find that the estimate of the local precipitation rate based

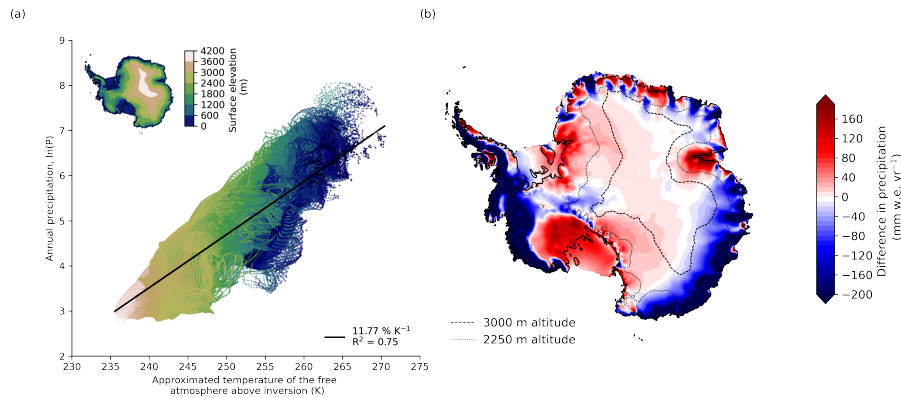


Figure 6. Antarctic precipitation determined by temperatures across the ice sheet. (a) Estimates of log-scaled precipitation against the temperature of the free atmosphere above the inversion, which is deduced from mean annual surface air temperatures for each grid point in the ERA5-land reanalysis (1981-2000 mean), using Eq. 2. (b) When assuming the simple spatial regression derived from panel (a) between precipitation and temperatures, reanalysed coastal precipitation is mostly underestimated (blue areas), while precipitation around Ross Ice Shelf is largely overestimated (red areas).

on a simple spatial regression with temperature agrees particularly well with observations in the East Antarctic plateau above 3000 m altitude, see Fig. 6 (b). In contrast, large differences between estimated and observed precipitation are prevalent in particular in the coastal regions.

320 The Southern Ocean system is additionally affected by large-scale variability in atmospheric conditions, for example changing storm tracks or changing pressure systems (Bromwich et al., 2004; Eayrs et al., 2021). Especially in West Antarctica, studies suggest a strong ENSO imprint on precipitation (Garreaud and Battisti, 1999; Bromwich et al., 2004; Nicolas et al., 2017). This underlines the necessity for incorporating ice sheets as coupled components into Earth-System Models, to explicitly be able to calculate the resulting interactions. This is particularly the case for multi-millennial integrations. While e.g. storm surges are
 325 affecting Antarctic precipitation on short timescales and on regional scale, we expect thermodynamic changes to dominate the integrated changes in precipitation. One could therefore argue that constraining the expected horizontal and vertical distribution of future warming above the Antarctic continent should therefore have highest priority in model development.

Another factor that affects the robustness of the estimated scaling factors from surface temperature is related to the structure of the atmosphere. As discussed above, when analysing model output, we can directly assess the relationship between surface
 330 temperature (or the temperature at any other level if we so wished) and precipitation, because the model explicitly calculate the humidity and temperature of any atmospheric layer that carries the moisture. When using the Clausius-Clapeyron equation directly to estimate scaling factors, we need to parameterise the relationship between surface temperature and the temperature of the moisture holding layer. This is particularly challenging in Antarctica, where the vertical temperature profile does not follow a simple adiabatic (or moist-adiabatic) profile, but is instead characterised by a pronounced inversion. The impact of this
 335 inversion can be approximated by Eq. 2, which then allows us to estimate the temperature of the moisture holding layer from

surface temperature for a typical inversion profile. As the inversion structure is not constant, some uncertainty is introduced into our estimates of the scaling factor by using this approximation for all our calculations. In addition, we can expect the inversion structure to weaken over time, as increasing CO₂ levels in the atmosphere weakens the radiative cooling in the atmosphere that contributes to the intensification of the temperature inversion with elevation.

340 Another explanation for the lower sensitivity factors than the theory suggest could be potential evaporation constraints, as suggested for instance by Li et al. (2013). Analysing CMIP5 model data, they find that precipitation increases with temperature globally only between 1.5 and 3 % K⁻¹. They conclude that one must take into account the energetic constraints on evaporation (approx. 1% – 4 % K⁻¹ in the range of 0°C–30°C) when analysing the precipitation scaling globally. We find however that our results do not differ much when analysing net precipitation (precipitation minus evaporation) versus precipitation as done
345 here.

Following Eq. 1 we could see a slight decrease in sensitivity factors across the ice sheet depending on the chosen warming scenario in Section 4. This is also apparent when repeating the spatial regression analysis for each year from 1850 to the end of the 21st century (23rd century, where data is available): we find that the 20-year running mean sensitivity declines by -0.064 (± 0.045), -0.060 (± 0.036) or -0.065 (± 0.039) points per degree of temperature rise in the SSP1-26, SSP2-45 and SSP5-85
350 scenario respectively (see Appendix Fig. A5). This decrease in sensitivity over time is especially strong for the simulations extending until year 2300. The low sensitivity in a warmer climate is consistent with the theory of Clausius-Clapeyron, as in colder conditions, for instance in large parts of East Antarctica, the increase of the moisture holding capacity with warming should be higher.

For the forcing of ice-sheet models, which typically rely on a fixed parameterization with a single sensitivity factor for all
355 temperature ranges, we therefore suggest to introduce temperature-dependent scaling factors, especially for high-end sea-level rise simulations. How well a new precipitation scaling parameterization in ice-sheet models performs compared to direct input by regional or global climate modes still needs to be further tested. When performing ice-sheet model simulations with this new set of sensitivity factors, it would be recommended to include a thorough discussion on the uncertainties arising from the scaling relationship, especially in the coastal areas.

360 Whether – and on which timescales – increased snowfall can offset dynamical ice loss from the Antarctic Ice Sheet in the future remains very uncertain. For such analysis, one must in particular consider the feedback that snowfall has on the general ice dynamics, since it is known that increased snowfall at the ice-sheet margins enhances the ice flow and thus the ice discharge across the grounding line (Winkelmann et al., 2012). Garbe et al. (2020), using exponentially scaled precipitation, show that despite an increase in surface mass balance, large parts of the Antarctic Ice Sheet could disintegrate on the long-term, with
365 a first critical warming threshold at around 2°C of global warming above pre-industrial, where the West Antarctic Ice Sheet might become unstable. This means that ice losses, further accelerated by the marine ice sheet instability (see e.g. Robel et al., 2019), cannot be compensated by additional snowfall as previously assumed. The assumption that increased snowfall directly translates into an increase in surface mass balance in the future can be further contested by studies investigating the non-linear growth in melt and runoff under warming (Gilbert and Kittel, 2021; van Wessem et al., 2023). Accumulation processes are
370 complex and with increasing melt of snow and of the subsequent firn layer, increased precipitation does not necessarily lead

to a mass gain in all parts of Antarctica. Given the present-day temperature conditions, most precipitation falls as snow in Antarctica. With ongoing warming however, rainfall will likely increase in amount, frequency and intensity along the coast of Antarctica over the next 80 years (Vignon et al., 2021). If more precipitation falls as liquid rain, the remaining water on the ice-sheet surface may amplify ongoing surface melt processes through the reduction of surface albedo, latent heat release or
375 hydro-fracturing (Kopp et al., 2017).

For future projections, it will remain important to approximate precipitation increases through temperature-scaling approaches, as coupled simulations with regional climate models remain computationally expensive, especially on multi-centennial timescales. Our results show that these scaling approaches can in principle capture the overall changes of precipitation in a warming world sufficiently well - however, when using a precipitation-scaling approach in ice-sheet modelling studies, the scal-
380 ing parameter needs to be chosen according to the given application, and its choice should potentially reflect the more complex temperature-dependency outlined here. In particular, our results suggest that Antarctic mass balance projections with uniform estimates of the scaling factor might overestimate the compensating effect of additional snowfall under future warming.

Data availability. The CMIP6 data used for this study are freely available from the Earth System Grid Federation (ESGF). We further want to thank the respective authors for providing the RACMO2.3 data. The spatial maps of the temperature sensitivity from Figures 4 are available
385 upon request.

Appendix A: Additional figures to the sensitivity analysis

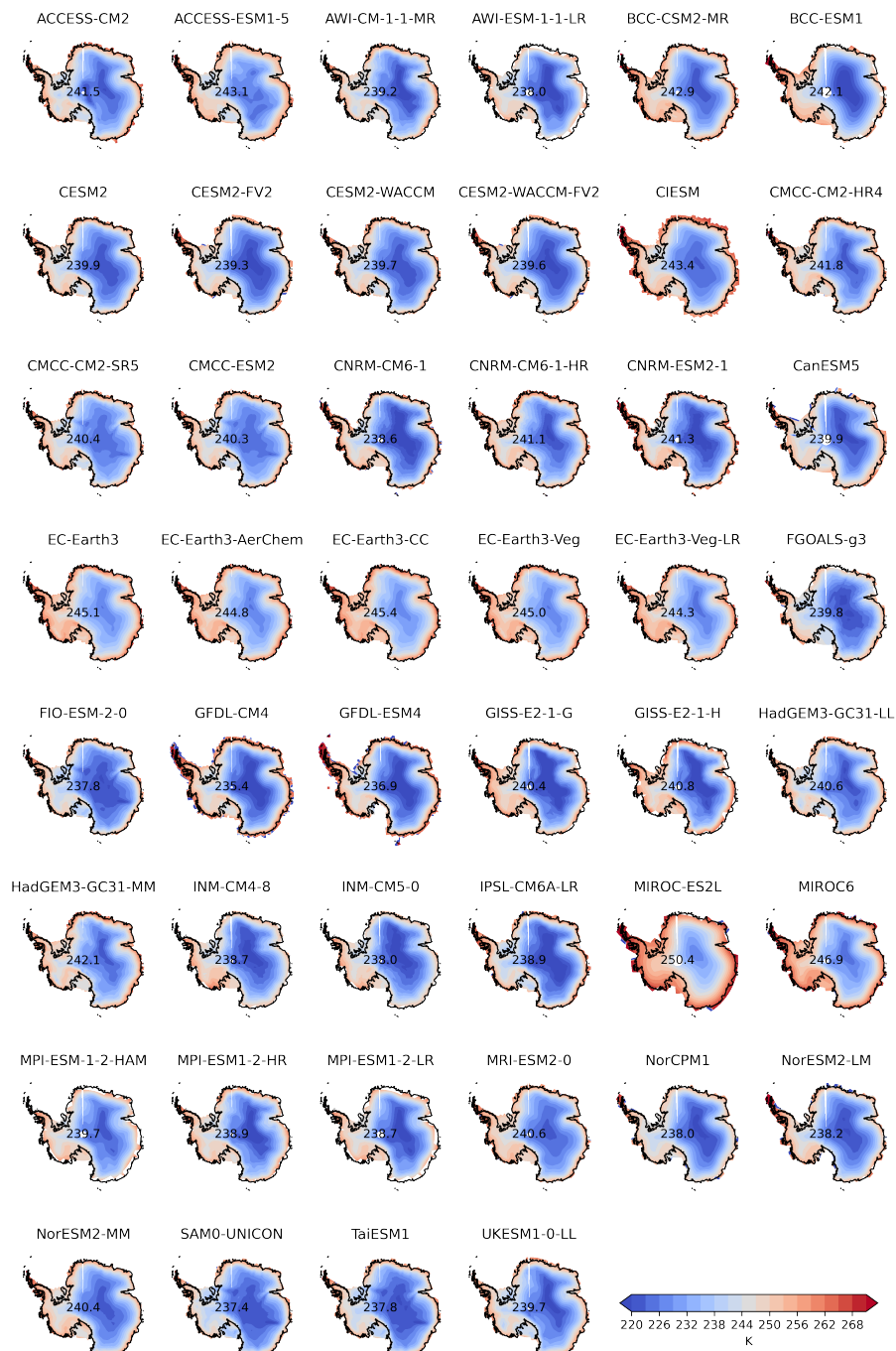


Figure A1. Mean annual air temperature for present-day conditions (1981-2000) from the CMIP6 model ensemble.

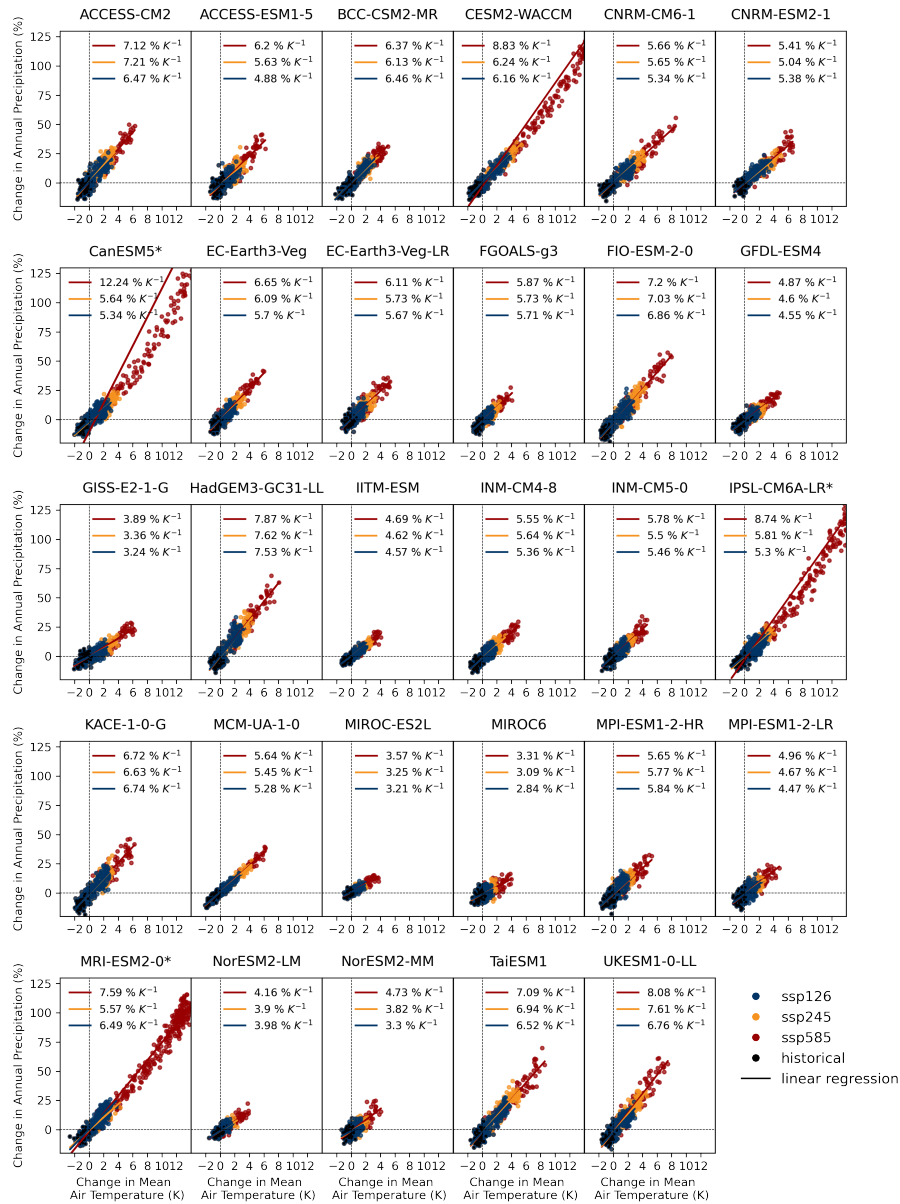


Figure A2. Models indicated with * simulate Antarctic climate change up to the year 2300. For the temporal regression analysis the full available time series were used.

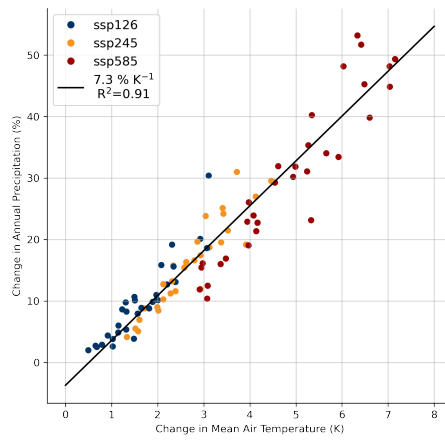


Figure A3. Each dot represents an individual model result on how much Antarctic precipitation and temperature has changed between the end of the 20th-century (1981-2000) and the end of the 21st-century (2081-2100).

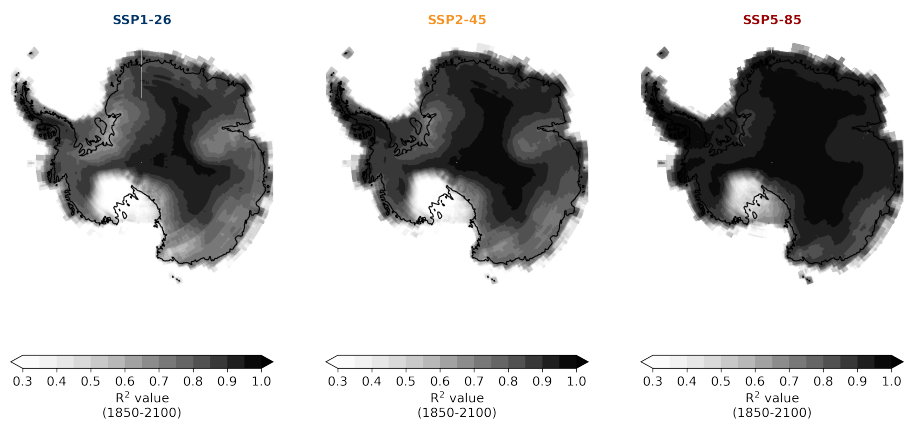


Figure A4. R^2 -values of performed grid-point-wise temporal regression using the CMIP6 ensemble mean of the different SSP-scenarios SSP1-26, SSP2-45 and SSP5-85 (1950-2100).

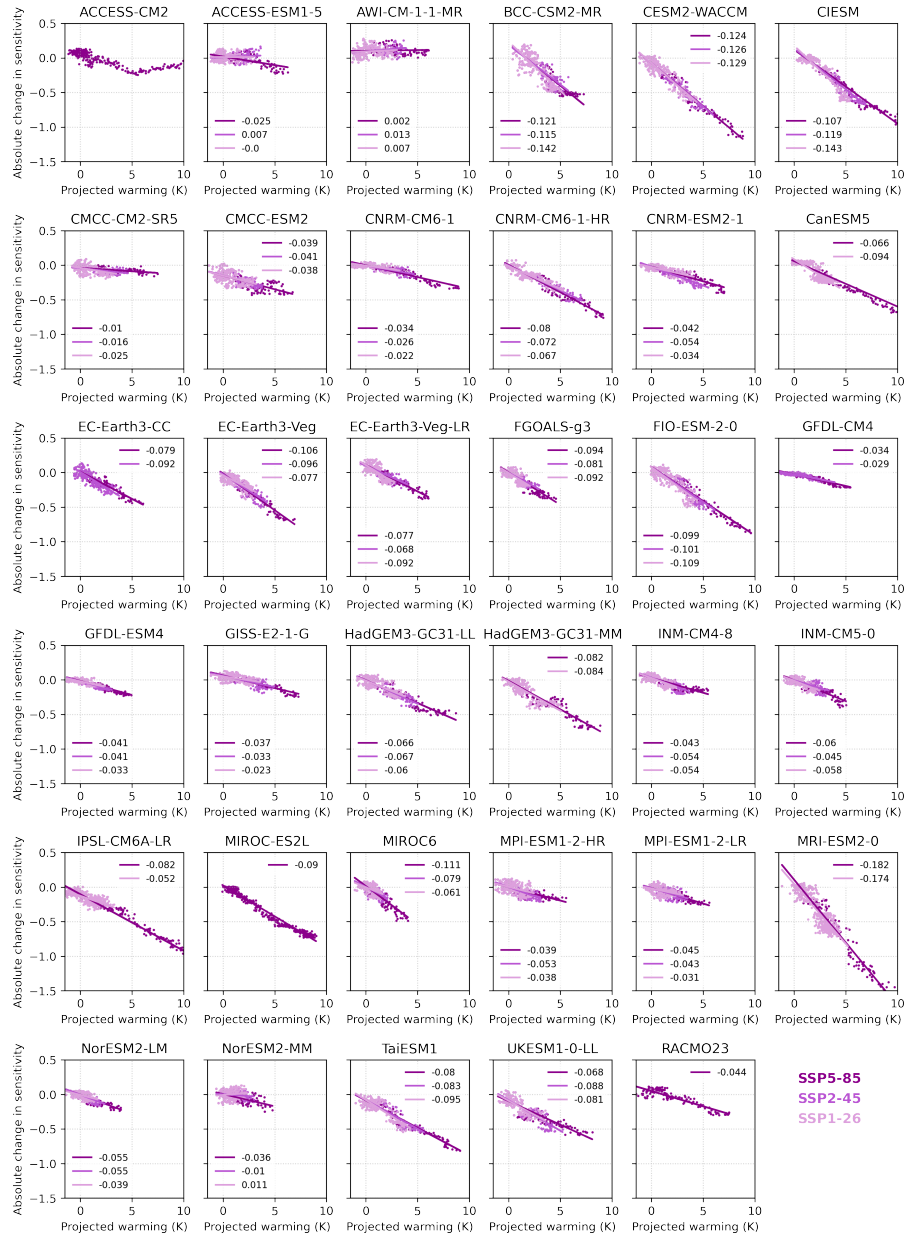


Figure A5. Decrease in sensitivity factor from spatial regression with warming. In most models we find for rising temperatures a strong decrease in the sensitivity of Antarctic precipitation to local air temperatures. Results are based on the entire time-series available for each of the individual models.

Author contributions. All authors designed the study. LN analysed the data and produced the figures. LN drafted the manuscript with strong support by RW.

Competing interests. The authors declare that they have no conflict of interest.

390 *Acknowledgements.* LN was supported by stipends by the Potsdam Graduate School and the Studienstiftung des Deutschen Volkes. LN and
RW gratefully acknowledge support by the European Union’s Horizon 2020 research and innovation programme under Grant Agreement
No. 820575 (TiPACCs). RW further acknowledges support by the European Union’s Horizon 2020 under Grant Agreement No. 869304
(PROTECT), by Deutsche Forschungsgemeinschaft (DFG) through grants WI4556/3-1 and WI4556/5-1 and by the PalMod project (FKZ:
01LP1925D), supported by the German Federal Ministry of Education and Research (BMBF) as a Research for Sustainability initiative
395 (FONA). DN acknowledges funding by the Deutsche Forschungsgemeinschaft (DFG) under Germany’s Excellence Strategy – EXC 2037
'CLICCS - Climate, Climatic Change, and Society' – Project Number: 390683824. We carried out our analyses on Mistral, the supercomputer
of the German Climate Computing Center (Deutsches Klimarechenzentrum, DKRZ) and its successor Levante.

References

- Agosta, C., Favier, V., Krinner, G., Gallée, H., Fettweis, X., and Genthon, C.: High-resolution modelling of the Antarctic surface mass balance, application for the twentieth, twenty first and twenty second centuries, *Climate dynamics*, 41, 3247–3260, <https://doi.org/10.1007/s00382-013-1903-9>, 2013.
- Albrecht, T., Winkelmann, R., and Levermann, A.: Glacial-cycle simulations of the Antarctic Ice Sheet with the Parallel Ice Sheet Model (PISM)–Part 2: Parameter ensemble analysis, *The Cryosphere*, 14, 633–656, <https://doi.org/10.5194/tc-14-633-2020>, 2020.
- Bengtsson, L., Hodges, K. I., Koumoutsaris, S., Zahn, M., and Keenlyside, N.: The changing atmospheric water cycle in polar regions in a warmer climate, *Tellus A: Dynamic meteorology and oceanography*, 63, 907–920, <https://doi.org/10.1111/j.1600-0870.2011.00534.x>, 2011.
- Bracegirdle, T. J., Connolley, W. M., and Turner, J.: Antarctic climate change over the twenty first century, *Journal of Geophysical Research: Atmospheres*, 113, <https://doi.org/10.1029/2007JD008933>, 2008.
- Bromwich, D. H.: Snowfall in high southern latitudes, *Reviews of Geophysics*, 26, 149–168, <https://doi.org/10.1029/RG026i001p00149>, 1988.
- Bromwich, D. H., Monaghan, A. J., and Guo, Z.: Modeling the ENSO modulation of Antarctic climate in the late 1990s with the Polar MM5, *Journal of climate*, 17, 109–132, 2004.
- Clapeyron, É.: Mémoire sur la puissance motrice de la chaleur, *Journal de l'École polytechnique*, 14, 153–190, 1834.
- Clausius, R.: Ueber die bewegende Kraft der Wärme und die Gesetze, welche sich daraus für die Wärmelehre selbst ableiten lassen, *Annalen der Physik*, 155, 368–397, <https://doi.org/10.1002/andp.18501550306>, 1850.
- Connolley, W.: The Antarctic temperature inversion, *International Journal of Climatology: A Journal of the Royal Meteorological Society*, 16, 1333–1342, [https://doi.org/10.1002/\(SICI\)1097-0088\(199612\)16:12<1333::AID-JOC96>3.0.CO;2-6](https://doi.org/10.1002/(SICI)1097-0088(199612)16:12<1333::AID-JOC96>3.0.CO;2-6), 1996.
- Donat-Magnin, M., Jourdain, N. C., Kittel, C., Agosta, C., Amory, C., Gallée, H., Krinner, G., and Chekki, M.: Future surface mass balance and surface melt in the Amundsen sector of the West Antarctic Ice Sheet, *The Cryosphere*, 15, 571–593, <https://doi.org/10.5194/tc-15-571-2021>, 2021.
- Eayrs, C., Li, X., Raphael, M. N., and Holland, D. M.: Rapid decline in Antarctic sea ice in recent years hints at future change, *Nature Geoscience*, 14, 460–464, 2021.
- Fortuin, J. and Oerlemans, J.: Parameterization of the annual surface temperature and mass balance of Antarctica, *Annals of Glaciology*, 14, 78–84, 1990.
- Fox-Kemper, B., Hewitt, H. T., Xiao, C., Aðalgeirsdóttir, G., Drijfhout, S. S., Edwards, T. L., Gолledge, N. R., Hemer, M., Kopp, R. E., Krinner, G., Mix, A., Notz, D., Nowicki, S., Nurhati, I. S., Ruiz, L., Sallée, J.-B., Slangen, A. B. A., and Yu, Y.: *Ocean, Cryosphere and Sea Level Change*, chap. 9, Cambridge University Press, Cambridge, United Kingdom and New York, NY, USA, in press, 2021.
- Frieler, K., Clark, P. U., He, F., Buizert, C., Reese, R., Ligtenberg, S. R., Van Den Broeke, M. R., Winkelmann, R., and Levermann, A.: Consistent evidence of increasing Antarctic accumulation with warming, *Nature Climate Change*, 5, 348–352, <https://doi.org/10.1038/nclimate2574>, 2015.
- Fudge, T., Markle, B. R., Cuffey, K. M., Buizert, C., Taylor, K. C., Steig, E. J., Waddington, E. D., Conway, H., and Koutnik, M.: Variable relationship between accumulation and temperature in West Antarctica for the past 31,000 years, *Geophysical Research Letters*, 43, 3795–3803, <https://doi.org/10.1002/2016GL068356>, 2016.

- Garbe, J., Albrecht, T., Levermann, A., Donges, J. F., and Winkelmann, R.: The hysteresis of the Antarctic ice sheet, *Nature*, 585, 538–544, 435 <https://doi.org/10.1038/s41586-020-2727-5>, 2020.
- Garreaud, R. and Battisti, D. S.: Interannual (ENSO) and interdecadal (ENSO-like) variability in the Southern Hemisphere tropospheric circulation, *Journal of Climate*, 12, 2113–2123, 1999.
- Gottelman, A., Hannay, C., Bacmeister, J. T., Neale, R. B., Pendergrass, A., Danabasoglu, G., Lamarque, J.-F., Fasullo, J., Bailey, D., Lawrence, D., et al.: High climate sensitivity in the Community Earth System Model version 2 (CESM2), *Geophysical Research Letters*, 440 46, 8329–8337, 2019.
- Gilbert, E. and Kittel, C.: Surface melt and runoff on Antarctic ice shelves at 1.5 C, 2 C, and 4 C of future warming, *Geophysical Research Letters*, 48, <https://doi.org/10.1029/2020GL091733>, 2021.
- Golledge, N. R., Kowalewski, D. E., Naish, T. R., Levy, R. H., Fogwill, C. J., and Gasson, E. G.: The multi-millennial Antarctic commitment to future sea-level rise, *Nature*, 526, 421–425, <https://doi.org/10.1038/nature15706>, 2015.
- 445 Grazioli, J., Madeleine, J.-B., Gallée, H., Forbes, R. M., Genthon, C., Krinner, G., and Berne, A.: Katabatic winds diminish precipitation contribution to the Antarctic ice mass balance, *Proceedings of the National Academy of Sciences*, 114, 10858–10863, <https://doi.org/10.1073/pnas.1707633114>, 2017.
- Gregory, J. and Huybrechts, P.: Ice-sheet contributions to future sea-level change, *Philosophical Transactions of the Royal Society A: Mathematical, Physical and Engineering Sciences*, 364, 1709–1732, <https://doi.org/10.1073/pnas.1817205116>, 2006.
- 450 Grieger, J., Leckebusch, G. C., and Ulbrich, U.: Net precipitation of Antarctica: Thermodynamical and dynamical parts of the climate change signal, *Journal of Climate*, 29, 907–924, <https://doi.org/10.1175/JCLI-D-14-00787.1>, 2016.
- Hartmann, D. L.: *Global Physical Climatology*, Elsevier, <https://doi.org/10.1016/C2009-0-00030-0>, 2016.
- Hausfather, Z., Marvel, K., Schmidt, G. A., Nielsen-Gammon, J. W., and Zelinka, M.: Climate simulations: Recognize the ‘hot model’ problem, <https://doi.org/10.1038/d41586-022-01192-2>, 2022.
- 455 Held, I. M. and Soden, B. J.: Robust responses of the hydrological cycle to global warming, *Journal of climate*, 19, 5686–5699, <https://doi.org/10.1175/JCLI3990.1>, 2006.
- Huybrechts, P.: Sea-level changes at the LGM from ice-dynamic reconstructions of the Greenland and Antarctic ice sheets during the glacial cycles, *Quaternary Science Reviews*, 21, 203–231, [https://doi.org/10.1016/S0277-3791\(01\)00082-8](https://doi.org/10.1016/S0277-3791(01)00082-8), 2002.
- IMBIE Team: Mass balance of the Antarctic Ice Sheet from 1992 to 2017, *Nature*, 558, 219–222, <https://doi.org/10.1038/s41586-018-0179-y>, 460 2018.
- Jouzel, J. and Merlivat, L.: Deuterium and oxygen 18 in precipitation: Modeling of the isotopic effects during snow formation, *Journal of Geophysical Research: Atmospheres*, 89, 11 749–11 757, 1984.
- Kittel, C., Amory, C., Agosta, C., Jourdain, N. C., Hofer, S., Delhasse, A., Doutreloup, S., Huot, P.-V., Lang, C., Fichet, T., et al.: Diverging future surface mass balance between the Antarctic ice shelves and grounded ice sheet, *The Cryosphere*, 15, 1215–1236, 465 <https://doi.org/10.5194/tc-15-1215-2021>, 2021.
- Kopp, R. E., DeConto, R. M., Bader, D. A., Hay, C. C., Horton, R. M., Kulp, S., Oppenheimer, M., Pollard, D., and Strauss, B. H.: Evolving understanding of Antarctic ice-sheet physics and ambiguity in probabilistic sea-level projections, *Earth’s Future*, 5, 1217–1233, <https://doi.org/10.1002/2017EF000663>, 2017.
- Krinner, G., Magand, O., Simmonds, I., Genthon, C., and Dufresne, J.-L.: Simulated Antarctic precipitation and surface mass balance at the 470 end of the twentieth and twenty-first centuries, *Climate Dynamics*, 28, 215–230, <https://doi.org/10.1007/s00382-006-0177-x>, 2007.

- Krinner, G., Llargeron, C., Ménégoz, M., Agosta, C., and Brutel-Vuilmet, C.: Oceanic forcing of Antarctic climate change: A study using a stretched-grid atmospheric general circulation model, *Journal of Climate*, 27, 5786–5800, <https://doi.org/10.1175/JCLI-D-13-00367.1>, 2014.
- 475 Lemonnier, F., Madeleine, J.-B., Claud, C., Palerme, C., Genthon, C., L'Ecuyer, T., and Wood, N. B.: CloudSat-inferred vertical structure of snowfall over the Antarctic continent, *Journal of Geophysical Research: Atmospheres*, 125, e2019JD031399, <https://doi.org/10.1029/2019JD031399>, 2019.
- Levermann, A., Clark, P. U., Marzeion, B., Milne, G. A., Pollard, D., Radic, V., and Robinson, A.: The multimillennial sea-level commitment of global warming, *Proceedings of the National Academy of Sciences*, 110, 13 745–13 750, <https://doi.org/10.1073/pnas.1219414110>, 2013.
- 480 Li, G., Harrison, S. P., Bartlein, P. J., Izumi, K., and Colin Prentice, I.: Precipitation scaling with temperature in warm and cold climates: an analysis of CMIP5 simulations, *Geophysical Research Letters*, 40, 4018–4024, <https://doi.org/10.1002/grl.50730>, 2013.
- Ligtenberg, S., Van de Berg, W., Van den Broeke, M., Rae, J., and Van Meijgaard, E.: Future surface mass balance of the Antarctic ice sheet and its influence on sea level change, simulated by a regional atmospheric climate model, *Climate dynamics*, 41, 867–884, <https://doi.org/10.1007/s00382-013-1749-1>, 2013.
- 485 MacLennan, M. L., Lenaerts, J. T., Shields, C., and Wille, J. D.: Contribution of Atmospheric Rivers to Antarctic Precipitation, *Geophysical Research Letters*, <https://doi.org/10.1029/2022GL100585>, 2022.
- Masson-Delmotte, V., Zhai, P., Pirani, A., Connors, S., Péan, C., Berger, S., Caud, N., Chen, Y., Goldfarb, L., Gomis, M., Huang, M., Leitzell, K., Lonnoy, E., Matthews, J., Maycock, T., Waterfield, T., Yelekçi, O., Yu, R., and Zhou, B., eds.: *Climate Change 2021: The Physical Science Basis. Contribution of Working Group I to the Sixth Assessment Report of the Intergovernmental Panel on Climate Change*, 490 Cambridge University Press, in press, 2021.
- Medley, B. and Thomas, E.: Increased snowfall over the Antarctic Ice Sheet mitigated twentieth-century sea-level rise, *Nature Climate Change*, 9, 34–39, <https://doi.org/10.1038/s41558-018-0356-x>, 2019.
- Meehl, G. A., Senior, C. A., Eyring, V., Flato, G., Lamarque, J.-F., Stouffer, R. J., Taylor, K. E., and Schlund, M.: Context for interpreting equilibrium climate sensitivity and transient climate response from the CMIP6 Earth system models, *Science Advances*, 6, eaba1981, 495 <https://doi.org/10.1126/sciadv.aba1981>, 2020.
- Monaghan, A. J., Bromwich, D. H., Fogt, R. L., Wang, S.-H., Mayewski, P. A., Dixon, D. A., Ekaykin, A., Frezzotti, M., Goodwin, I., Isaksson, E., et al.: Insignificant change in Antarctic snowfall since the International Geophysical Year, *Science*, 313, 827–831, <https://doi.org/10.1126/science.1128243>, 2006.
- Mottram, R., Hansen, N., Kittel, C., Van Wessem, J. M., Agosta, C., Amory, C., Boberg, F., Van De Berg, W. J., Fettweis, X., Gossart, A., 500 Van Lipzig, N. P., Van Meijgaard, E., Orr, A., Phillips, T., Webster, S., Simonsen, S. B., and Souverijns, N.: What is the surface mass balance of Antarctica? An intercomparison of regional climate model estimates, 15, 3751–3784, <https://doi.org/10.5194/tc-15-3751-2021>, 2021.
- Muszynski, I. and Birchfield, G.: The dependence of Antarctic accumulation rates on surface temperature and elevation, *Tellus A*, 37, 204–208, 1985.
- 505 Muñoz Sabater, J.: ERA5-Land monthly averaged data from 1981 to present, <https://cds.climate.copernicus.eu>, <https://doi.org/10.24381/cds.68d2bb3>, accessed: 2020-12-13, 2019.

- Nicolas, J. P., Vogelmann, A. M., Scott, R. C., Wilson, A. B., Cadet, M. P., Bromwich, D. H., Verlinde, J., Lubin, D., Russell, L. M., Jenkinson, C., et al.: January 2016 extensive summer melt in West Antarctica favoured by strong El Niño, *Nature communications*, 8, 1–10, <https://doi.org/10.1038/ncomms15799>, 2017.
- 510 Otosaka, I. N., Shepherd, A., Ivins, E. R., Schlegel, N.-J., Amory, C., van den Broeke, M., Horwath, M., Joughin, I., King, M., Krinner, G., et al.: Mass Balance of the Greenland and Antarctic Ice Sheets from 1992 to 2020, *Earth System Science Data Discussions*, pp. 1–33, <https://doi.org/10.5194/essd-2022-261>, 2022.
- Palermo, C., Kay, J., Genthon, C., L'Ecuyer, T., Wood, N., and Claud, C.: How much snow falls on the Antarctic ice sheet?, *The Cryosphere*, 8, 1577–1587, <https://doi.org/10.5194/tc-8-1577-2014>, 2014.
- 515 Palermo, C., Genthon, C., Claud, C., Kay, J. E., Wood, N. B., and L'Ecuyer, T.: Evaluation of current and projected Antarctic precipitation in CMIP5 models, *Climate dynamics*, 48, 225–239, <https://doi.org/10.1007/s00382-016-3071-1>, 2017.
- Parish, T. R. and Bromwich, D. H.: Reexamination of the near-surface airflow over the Antarctic continent and implications on atmospheric circulations at high southern latitudes, *Monthly Weather Review*, 135, 1961–1973, <https://doi.org/10.1175/MWR3374.1>, 2007.
- Payne, A. J., Nowicki, S., Abe-Ouchi, A., Agosta, C., Alexander, P., Albrecht, T., Asay-Davis, X., Aschwendon, A., Barthel, A., Bracegirdle, T. J., et al.: Future sea level change under coupled model intercomparison project phase 5 and phase 6 scenarios from the Greenland and Antarctic ice sheets, *Geophysical Research Letters*, 48, e2020GL091741, <https://doi.org/10.1029/2020GL091741>, 2021.
- 520 Petit, J.-R., Jouzel, J., Raynaud, D., Barkov, N. I., Barnola, J.-M., Basile, I., Bender, M., Chappellaz, J., Davis, M., Delaygue, G., et al.: Climate and atmospheric history of the past 420,000 years from the Vostok ice core, Antarctica, *Nature*, 399, 429–436, <https://doi.org/10.1038/20859>, 1999.
- 525 Quiquet, A., Dumas, C., Ritz, C., Peyaud, V., and Roche, D. M.: The GRISLI ice sheet model (version 2.0): calibration and validation for multi-millennial changes of the Antarctic ice sheet, *Geoscientific Model Development*, 11, 5003–5025, <https://doi.org/10.5194/gmd-11-5003-2018>, 2018.
- Riahi, K., Van Vuuren, D. P., Kriegler, E., Edmonds, J., O'neill, B. C., Fujimori, S., Bauer, N., Calvin, K., Dellink, R., Fricko, O., et al.: The shared socioeconomic pathways and their energy, land use, and greenhouse gas emissions implications: an overview, *Global Environmental Change*, 42, 153–168, <https://doi.org/10.1016/j.gloenvcha.2016.05.009>, 2017.
- 530 Rignot, E., Mouginot, J., and Scheuchl, B.: Ice flow of the Antarctic ice sheet, *Science*, 333, 1427–1430, <https://doi.org/10.1126/science.1208336>, 2011.
- Rignot, E., Mouginot, J., Scheuchl, B., Van Den Broeke, M., Van Wessem, M. J., and Morlighem, M.: Four decades of Antarctic Ice Sheet mass balance from 1979–2017, *Proceedings of the National Academy of Sciences*, 116, 1095–1103, <https://doi.org/10.1073/pnas.1812883116>, 2019.
- 535 Robel, A. A., Seroussi, H., and Roe, G. H.: Marine ice sheet instability amplifies and skews uncertainty in projections of future sea-level rise, *Proceedings of the National Academy of Sciences*, 116, 14887–14892, <https://doi.org/10.1073/pnas.1904822116>, 2019.
- Robin, G. d. Q.: Ice cores and climatic change, *Philosophical Transactions of the Royal Society of London. B, Biological Sciences*, 280, 143–168, <https://doi.org/10.1098/rstb.1977.0103>, 1977.
- 540 Rodehacke, C. B., Pfeiffer, M., Semmler, T., Gurses, Ö., and Kleiner, T.: Future sea level contribution from Antarctica inferred from CMIP5 model forcing and its dependence on precipitation ansatz, *Earth System Dynamics*, 11, 1153–1194, <https://doi.org/10.5194/esd-11-1153-2020>, 2020.
- Roussel, M.-L., Lemonnier, F., Genthon, C., and Krinner, G.: Brief communication: Evaluating Antarctic precipitation in ERA5 and CMIP6 against CloudSat observations, *The Cryosphere*, 14, 2715–2727, <https://doi.org/10.5194/tc-14-2715-2020>, 2020.

- 545 Seroussi, H., Nowicki, S., Payne, A. J., Goelzer, H., Lipscomb, W. H., Abe-Ouchi, A., Agosta, C., Albrecht, T., Asay-Davis, X., Barthel, A., et al.: ISMIP6 Antarctica: a multi-model ensemble of the Antarctic ice sheet evolution over the 21st century, *The Cryosphere*, 14, 3033–3070, <https://doi.org/10.5194/tc-14-3033-2020>, 2020.
- Sikka, D.: Desert climate and its dynamics, *Current Science*, pp. 35–46, <https://www.jstor.org/stable/24098628>, 1997.
- Uotila, P., Lynch, A. H., Cassano, J. J., and Cullather, R.: Changes in Antarctic net precipitation in the 21st century based
550 on Intergovernmental Panel on Climate Change (IPCC) model scenarios, *Journal of Geophysical Research: Atmospheres*, 112, <https://doi.org/10.1029/2006JD007482>, 2007.
- van Meijgaard, E., Van Ulft, L., Van de Berg, W., Bosveld, F., Van den Hurk, B., Lenderink, G., and Siebesma, A.: The KNMI regional atmospheric climate model RACMO, version 2.1, Citeseer, 2008.
- Van Ommen, T. D., Morgan, V., and Curran, M. A.: Deglacial and holocene changes in accumulation at Law Dome, East Antarctica, *Annals
555 of Glaciology*, 39, 359–365, 2004.
- Van Wessem, J. M., Van De Berg, W. J., Noël, B. P., Van Meijgaard, E., Amory, C., Birnbaum, G., Jakobs, C. L., Krüger, K., Lenaerts, J., Lhermitte, S., et al.: Modelling the climate and surface mass balance of polar ice sheets using RACMO2–Part 2: Antarctica (1979–2016), *The Cryosphere*, 12, 1479–1498, <https://doi.org/10.5194/tc-12-1479-2018>, 2018.
- van Wessem, J. M., van den Broeke, M. R., Wouters, B., and Lhermitte, S.: Variable temperature thresholds of melt pond formation on
560 Antarctic ice shelves, *Nature Climate Change*, pp. 1–6, 2023.
- Vignon, É., Roussel, M.-L., Gorodetskaya, I., Genthon, C., and Berne, A.: Present and Future of Rainfall in Antarctica, *Geophysical Research Letters*, 48, e2020GL092281, <https://doi.org/10.1029/2020GL092281>, 2021.
- Wille, J. D., Favier, V., Dufour, A., Gorodetskaya, I. V., Turner, J., Agosta, C., and Codron, F.: West Antarctic surface melt triggered by atmospheric rivers, *Nature Geoscience*, 12, 911–916, <https://doi.org/10.1038/s41561-019-0460-1>, 2019.
- 565 Winkelmann, R., Levermann, A., Martin, M. A., and Frieler, K.: Increased future ice discharge from Antarctica owing to higher snowfall, *Nature*, 492, 239–242, <https://doi.org/10.1038/nature11616>, 2012.
- Zelinka, M. D., Myers, T. A., McCoy, D. T., Po-Chedley, S., Caldwell, P. M., Ceppi, P., Klein, S. A., and Taylor, K. E.: Causes of higher climate sensitivity in CMIP6 models, *Geophysical Research Letters*, 47, e2019GL085782, <https://doi.org/10.1029/2019GL085782>, 2020.
- Zwally, H. J., Giovinetto, M. B., Beckley, M. A., and Saba, J. L.: Antarctic and Greenland drainage systems, GSFC cryospheric sciences
570 laboratory, 2012.
- Zwally, H. J., Li, J., Robbins, J. W., Saba, J. L., Yi, D., and Brenner, A. C.: Mass gains of the Antarctic ice sheet exceed losses, *Journal of Glaciology*, 61, 1019–1036, <https://doi.org/10.3189/2015JoG15J071>, 2015.

Table A1. Model-specific results. We perform a sensitivity analysis with the evolution of log-scaled mean annual precipitation and mean annual air temperature (both continent-wide estimates) over the time period 1850-2100 using different SSP-scenarios.

Model	hist + SSP1-26 (% K ⁻¹)	R ²	hist + SSP2-45 (% K ⁻¹)	R ²	hist + SSP5-85 (% K ⁻¹)	R ²
ACCESS-CM2	5.97	0.71	6.37	0.8	6.09	0.89
ACCESS-ESM1-5	4.39	0.5	5.08	0.66	5.14	0.85
BCC-CSM2-MR	6.26	0.82	5.92	0.8	5.89	0.89
CESM2-WACCM	5.85	0.85	5.77	0.89	5.64	0.94
CIESM	6.17	0.84	5.86	0.88	5.55	0.93
CMCC-CM2-SR5	7.01	0.71	6.85	0.8	6.68	0.88
CMCC-ESM2	6.85	0.75	6.73	0.81	6.56	0.9
CNRM-CM6-1	5.24	0.77	5.39	0.86	5.05	0.92
CNRM-CM6-1-HR	6.7	0.87	6.38	0.91	5.97	0.94
CNRM-ESM2-1	5.15	0.74	4.74	0.82	4.84	0.88
CanESM5	5.47	0.75	5.5	0.83	5.72	0.94
EC-Earth3-CC	n/a	n/a	5.64	0.68	5.95	0.81
EC-Earth3-Veg	5.61	0.62	5.84	0.76	6.01	0.88
EC-Earth3-Veg-LR	5.52	0.56	5.45	0.7	5.52	0.82
FGOALS-g3	5.76	0.63	5.69	0.73	5.64	0.84
FIO-ESM-2-0	6.9	0.8	6.8	0.87	6.43	0.93
GFDL-CM4	n/a	n/a	5.42	0.75	5.29	0.85
GFDL-ESM4	4.74	0.56	4.73	0.65	4.84	0.8
GISS-E2-1-G	3.72	0.62	3.68	0.74	3.9	0.87
HadGEM3-GC31-LL	7.14	0.76	7.01	0.85	6.72	0.91
HadGEM3-GC31-MM	7.33	0.83	n/a	n/a	6.71	0.92
INM-CM4-8	5.43	0.67	5.58	0.77	5.28	0.88
INM-CM5-0	5.38	0.64	5.32	0.76	5.36	0.85
IPSL-CM6A-LR	5.07	0.67	5.5	0.81	5.31	0.9
MIROC-ES2L	3.22	0.52	3.18	0.6	3.4	0.78
MIROC6	2.78	0.2	2.95	0.31	3.29	0.54
MPI-ESM1-2-HR	5.78	0.55	5.63	0.68	5.29	0.78
MPI-ESM1-2-LR	4.48	0.4	4.62	0.56	4.75	0.73
MRI-ESM2-0	5.35	0.72	5.39	0.79	5.42	0.89
NorESM2-LM	4.22	0.44	4.1	0.56	4.19	0.73
NorESM2-MM	3.36	0.26	3.85	0.39	4.59	0.64
TaiESM1	6.41	0.8	6.51	0.85	6.16	0.92
UKESM1-0-LL	6.73	0.73	7.23	0.84	7.08	0.9
CMIP6 model mean	5.48	0.65	5.46	0.74	5.46	0.85
RACMO2.3	n/a	n/a	n/a	n/a	6.37	0.92